

Calcium-Sensing Receptor Stimulation Induces Nonselective Cation Channel Activation in Breast Cancer Cells

Yassine El Hiani¹, Ahmed Ahidouch^{1,2}, Morad Roudbaraki³, Stéphanie Guenin⁴, Gérard Brûlé¹, Halima Ouadid-Ahidouch¹

¹Laboratoire de Physiologie Cellulaire et Moléculaire, EA 2086, Faculté des Sciences, Université de Picardie Jules Verne, 33 rue Saint-leu, 80039 Amiens, France

²Laboratoire de Physiologie Animale, Faculté des Sciences, Université Ibn-Zohr, BP 28/S, 80000 Agadir, Morocco

³INSERM EMI 0228, Université de Lille, 59655 Villeneuve d'Ascq, France

⁴Centre de Ressources Régionales en Biologie Moléculaire, Université de Picardie Jules Verne, 10 rue Baudeloque, 80039 Amiens, Cedex 1, France

Received: 24 March 2006/Revised: 30 June 2006

Abstract. The calcium-sensing receptor (CaR) is expressed in epithelial ducts of both normal human breast and breast cancer tissue, as well as in the MCF-7 cell line as assessed by immunohistochemistry and Western blot analysis. However, to date, there are no data regarding the transduction pathways of CaR in breast cancer cells. In this study, we show that a CaR agonist, spermine, and increased extracellular Ca^{2+} ($[\text{Ca}^{2+}]_o$) sequentially activate two inward currents at -80 mV. The first was highly permeable to Ca^{2+} and inhibited by 2-aminophenyl borate (2-APB). In contrast, the second was more sensitive to Na^+ and Li^+ than to Ca^{2+} and insensitive to 2-APB. Furthermore, intracellular dialysis with high Mg^{2+} , flufenamic acid or amiloride perfusion was without any effect on the second current. Both currents were inhibited by La^{3+} . Calcium imaging recordings showed that both $[\text{Ca}^{2+}]_o$ and spermine induced an increase in intracellular calcium ($[\text{Ca}^{2+}]_i$) and that removal of extracellular Ca^{2+} or perfusion of 2-APB caused a decline in $[\text{Ca}^{2+}]_i$. It is well known that stimulation of CaR by an increase in $[\text{Ca}^{2+}]_o$ or with spermine is associated with activation of phospholipase C (PLC). Inhibition of PLC reduced the $[\text{Ca}^{2+}]_o$ -stimulated $[\text{Ca}^{2+}]_i$ increase. Lastly, reverse-transcriptase polymerase chain reaction showed that MCF-7 cells expressed canonical transient receptor potential (TRPCs) channels. Our results suggest that, in MCF-

7 cells, CaR is functionally coupled to Ca^{2+} -permeable cationic TRPCs, for which TRPC1 and TRPC6 are the most likely candidates for the highly selective Ca^{2+} current. Moreover, the pharmacology of the second Na^+ current excludes the involvement of the more selective Na^+ transient receptor potential melastatin (TRPM4 and TRPM5) and the classical epithelial Na^+ channels.

Key words: Calcium-sensing receptor — Cationic current — Transient receptor potential channel — Breast cancer cell

Introduction

Breast cancer is the most common cancer and a leading cause of cancer-associated death in women (Boring et al., 1994). It most commonly metastasizes to the bone, with 70% of patients dying of breast carcinoma having bone metastases (Mundy, 1997). Consequently, tumors induce bone resorption and lead to the release of large quantities of Ca^{2+} into the bone microenvironment. The local Ca^{2+} level at resorption sites has been reported to rise as high as 40 mM (Silver, Murrills & Etherington, 1988). It has been reported that high Ca^{2+} concentrations stimulate the calcium-sensing receptor (CaR), thereby inducing parathormone-related peptide (PTHrP) production by MCF-7 and MDA-MB-231 breast cancer cells (Sanders et al., 2000). High levels of PTHrP contribute to increased bone resorption and to the osteolysis observed in association with metastasis of epithelium-derived tumors to bone (Rodland,

This work concretizes the scientific cooperation between Université de Picardie Jules Verne and Université Ibn-Zohr.

Correspondence to: Halima Ouadid-Ahidouch; email: ha-sciences@u-picardie.fr

2004). The potential role of CaR in modulating PTHrP secretion has been investigated in breast cancer (Sanders et al., 2000), prostate cancer (Sanders et al., 2001), glial tumors (Chattopadhyay et al., 2000) and Leydig cell tumors (Buchs et al., 2000). Recently, Li, Huang & Peng (2005) reported overexpression of CaR in some cancer tissues and suggested that CaR may play a role in cancer progression.

CaR is a G protein-coupled receptor, originally cloned from bovine parathyroid cells (Brown et al., 1993), which plays an important role in the maintenance of systemic Ca^{2+} homeostasis. It has been reported that CaR stimulation by an increase in extracellular Ca^{2+} concentration ($[\text{Ca}^{2+}]_o$) or a polyamine (spermine) is associated with activation of phospholipase C (PLC) (Huang, Handlogten & Miller, 2002) and increases the levels of intracellular inositol 1,4,5-trisphosphate (IP_3) (Guise et al., 1996). It is well known that PLC cleaves phosphatidylinositol 4,5-bisphosphate into IP_3 and diacylglycerol (DAG). IP_3 releases Ca^{2+} from intracellular stores, and the concomitant store depletion activates store-operated Ca^{2+} channels (SOCs), which in many cases have been tentatively identified as transient receptor potential (TRP) family members (Zitt, Halaszovich & Luckhoff, 2002; Pedersen, Owsianik & Nilius, 2005; Parekh & Putney, 2005). Moreover, DAG is also capable of activating some other TRPs directly, without depleting intracellular Ca^{2+} stores (Pedersen et al., 2005).

In breast cells, CaR stimulation induces an increase in intracellular Ca^{2+} concentration ($[\text{Ca}^{2+}]_i$) (Parkash, Chaudhry & Rhoten, 2004) as well as PTHrP secretion (Sanders et al., 2000). Furthermore, a cationic nonselective current has been recorded both in response to CaR stimulation in hippocampal neurons (Ye et al., 1996a, 1997) and in HEK293 cells stably transfected with human CaR (Ye et al., 1996b). The greater incidence of this cationic current has been associated with U373 human astrocytoma cell proliferation (Chattopadhyay et al., 2000) and with differentiation of human promyelocytic leukemia cells (Yamaguchi et al., 2000). However, nothing is currently known about the pharmacological and electrophysiological properties of this cationic current and the link between the CaR and TRP channels (TRPCs).

We combined electrophysiological and molecular methods to demonstrate, for the first time, that both CaR agonists (spermine and Ca^{2+}) sequentially activate two cationic currents: a primary highly Ca^{2+} -sensitive current (I_1), which is always followed by a secondary highly Na^+ -sensitive stronger one (I_2). Furthermore, the pharmacological and electrophysiological properties of the primary current, on the one hand, and the transcripts of canonical TRPCs that we have found in MCF-7 cells, on the other hand, lead us to suggest that TRPC1 and/or TRPC6 might be candidates for the first current induced by the activation of CaR.

Materials and Methods

CELL CULTURE

MCF-7 cells between passages 149 and 210 were cultured in Eagle's minimum essential medium supplemented with 5% fetal calf serum, 2 mM L-glutamine and 0.06% 4-(2-hydroxyethyl)-1-piperazineethanesulfonic acid (HEPES) buffer and maintained at 37°C in a humid atmosphere of 5% CO_2 in air.

ELECTROPHYSIOLOGY

For electrophysiological analysis, cells were cultured in 35-mm Petri dishes at a density of 5×10^4 for 2 days before patch-clamp experiments. Currents were recorded in voltage-clamp mode, using an Axopatch 200 B patch-clamp amplifier and a Digidata 1200 interface (both from Axon Instruments, Burlingame, CA). PClamp software (v. 6.03, Axon Instruments) was used to control voltage as well as to acquire and analyze data. The whole-cell mode of the patch-clamp technique was used with 3–5 M Ω resistance borosilicate fire-polished pipettes (Hirschmann[®] Laborgerate, Eberstadt, Germany). Seal resistance was typically in the 10–20 G Ω range. The maximum uncompensated series resistance was < 10 M Ω during whole-cell recordings, so the voltage error was < 5 mV for a current amplitude of 500 pA. Recordings where series resistance resulted in errors > 5 mV in voltage commands were discarded. Whole-cell currents were allowed to stabilize for 5 min before being measured. Membrane capacitance was measured by voltage clamp with a voltage pulse after completion of a whole-cell patch-clamp procedure, and compensation of the electrode capacitance with electronic circuits was built into the patch-clamp amplifier. Results were expressed using current densities instead of current amplitude. The MCF-7 cell surface was thus estimated by measuring membrane capacitance (30 ± 1.7 pF, $n = 45$). Currents were recorded using the whole-cell patch-clamp technique during ramps from –80 to +80 mV, applied from a holding potential of –40 mV for 250 ms. The current value was measured at the end of the ramp protocol at –80 mV.

Cells were allowed to settle in Petri dishes placed at the opening of a 250- μm inner diameter capillary for extracellular perfusions. The cell under investigation was continuously superfused with control or test solutions. All electrophysiological experiments were performed at room temperature.

SOLUTIONS

External and internal solutions had the following compositions (in mM): external, NaCl 100, KCl 5, MgCl_2 1 and HEPES 10 at pH 7.4 (TEAOH); internal, CsCl 150, HEPES 10, ethyleneglycoltetraacetic acid (EGTA) 0.1 and MgCl_2 2 at pH 7.2 (CsOH). Extracellular and intracellular osmolarity values measured with a freezing-point depression were 300 and 292 mOs, respectively. In order to completely block K^+ channels, we added tetraethylammonium (TEA) at 20 mM to the extracellular medium. 2-Aminophenyl borate (2-APB), U73122 and U73343 (Sigma, Saint Quentin Fallavier, France) was made in dimethyl sulfoxide (DMSO). Final concentrations were obtained by appropriate dilution in an external control solution. The final concentration of DMSO was < 0.1%. For the Na^+ -free solution, Na^+ was replaced by choline and the pH was adjusted to 7.4 by TEOH.

STATISTICAL ANALYSIS

Results were expressed as mean \pm standard error (SE). Experiments were repeated at least three times. Student's *t*-test was used to compare treatment means with electrophysiological

Table 1. Sequences of selected oligonucleotides used as RT-PCR primers

Targets	Oligonucleotides sequences	Position in GenBank sequence (accession number)	Expected fragment size (bp)
hTRPC1	Forward: 5'- TTCCTCTCCATCCTCTTCCTCG-3' Reverse: 5'- CATAGTTGTTACGATGAGCAGC-3'	457–478 (Z73903)	458 for TRPC1, 356 for TRPC1A, 298 for TRPC1B
hTRPC3	Forward: 5'-TACTCAACATGCTAATTGCTATGAT-3' Reverse: 5'-CACAGTTGCTTGGCTCTGTCTTCC-3'	2147–2170 (U47050) 26192643 (U47050)	383 for TRPC3
hTRPC4	Forward: 5'-CTCTGGTTGTTCTACTCAACATG-3' Reverse: 5'-CCTGTTGACGAGCAACTTCTTCT-3'	2058–2082 (AF063822) 2861–2839 (AF063822)	781 for TRPC4
hTRPC6	Forward: 5'-GAACTTAGCAATGAACTGGCAGT-3' Reverse: 5'-CATATCATGCCTATTACCCAGGA-3'	1322–1345 (AJ006276) 1947–1925 (AJ006276)	625 for TRPC6, 277 for TRPC6 γ
hTRPC7	Forward: 5'-GTCCGAATGCAAGGAAATCT-3' Reverse: 5'-TGGGTTGTATTGGCACCTC-3'	1356–1375 (AJ272034) 1814–1834 (AJ272034)	477 for TRPC7

control means (paired *t*-test). *P* < 0.05 was considered significant.

CALCIUM MEASUREMENTS

MCF-7 cells were grown on glass coverslips for calcium imaging experiments. The cytosolic calcium concentration was measured using Fura-2-loaded cells. MCF-7 cells were loaded for 1 h at room temperature with 3.3 μ M Fura-2/AM prepared in saline solution and subsequently washed three times with the same dye-free solution. The coverslip was then transferred into a perfusion chamber of a Zeiss (Thornwood, NY) microscope equipped for fluorescence. Fluorescence was excited at 350 and 380 nm alternately, using a monochromator (Polychrome IV; TILL Photonics, Planegg, Germany), and captured by a Cool SNAP HQ camera (Princeton Instruments, Evry, France) after filtration through a long-pass filter (510 nm). Metafluor software (v. 6.2r6; Universal Imaging, West Chester, PA) was used for acquisition and analysis. All recordings were carried out at room temperature. The cells were continuously perfused with the saline solution, and chemicals were added via the perfusion system. The flow rate of the whole-chamber perfusion system was set at 1 ml/min, and the chamber volume was 500 μ l.

REVERSE-TRANSCRIPTASE POLYMERASE CHAIN REACTION ANALYSIS

Total RNA from MCF-7 cells was extracted by the guanidinium thiocyanate-phenol-chloroform procedure. After deoxyribonuclease I treatment (0.1 U/ μ l, 1 h at 25°C; Invitrogen, La Jolla, CA) to eliminate genomic DNA, total RNA was reverse-transcribed into cDNA. For polymerase chain reactions (PCRs), specific sense and antisense primers were designed, based on GenBank hTRP sequences, using GeneJockey II software (Biosoft, Cambridge, UK) as listed in Table 1. Primers were synthesized by Invitrogen. TRPC cDNA was amplified using Ampli-Taq Gold DNA Polymerase (Perkin-Elmer, Oak Brook, IL) in an automated thermal cycler (GenAmp 2400, Perkin-Elmer). DNA amplification conditions included an initial 7-min denaturation step at 95°C (which also activated the Taq Gold) and 40 cycles of 30 s at 95°C, 30 s at 58°C, 40 s–1 min (depending on the fragments amplified) at 72°C and final elongation of 7 min at 72°C. PCR products were electrophoresed on a 1.5–2% agarose gel and stained with ethidium bromide (0.5 μ g/ml), then visualized under ultraviolet light. In order to identify them, each PCR band was extracted from the gel and then subjected either to restriction analysis using the specific enzymes for each fragment amplified or subcloned in Taq-amplified-cloning (TA-cloning) vector (Invitrogen), followed by the sequencing analysis.

Results

CAR STIMULATION INDUCES TWO CATIONIC CURRENTS IN MCF-7 CELLS

Because the local Ca^{2+} concentration near resorbing osteoclasts may rise as high as 40 mM (Silver et al., 1988), metastatic tumor cells in bone could be exposed to very high Ca^{2+} levels. In this study, we tested the effects of 10 and 20 mM $[\text{Ca}^{2+}]_o$ on MCF-7 breast cancer cells, focusing on the regulation of calcium and sodium entry.

The two broad classes of CaR agonists, Ca^{2+} and spermine, were used. Experiments were performed on MCF-7 cells under conditions that ensured effective suppression of the K^+ currents characteristic of these cells (Ouadid-Ahidouch et al., 2004). Voltage ramps from -80 to +80 mV were applied every 30 s. Under our experimental conditions, these pulses elicited only a small background current. Exposing the cell to 20 mM $[\text{Ca}^{2+}]_o$ sequentially activated, at -80 mV, two inward currents (Fig. 1A). The primary current (I_1) reached a maximal steady state after about 5.9 ± 0.7 min ($n = 10$, Fig. 1A). The current density increased by 20 mM $[\text{Ca}^{2+}]_o$ from -3.8 ± 0.2 to -32.8 ± 2.6 pA/pF ($n = 12$) at -80 mV. The reversal potential (E_{rev}) was 5 ± 1 mV ($n = 10$, Fig. 1B), which is consistent with nonselective cation currents. A second current (I_2) was subsequently activated and increased rapidly in magnitude (Fig. 1A). The I_2 current density increased by 20 mM $[\text{Ca}^{2+}]_o$ from -3.8 ± 0.2 to -118 ± 8.2 pA/pF ($n = 13$) at -80 mV. Again, the reversal potential close to 0 mV (-4.8 ± 0.9 mV, $n = 8$; Fig. 1C) indicated that I_2 is nonselective within cations. The two inward currents were also developed in the presence of 1 mM spermine (Fig. 1D-F): the first increased from -3.3 ± 0.6 to -12 ± 1.2 pA/pF ($n = 20$, Fig. 1D), and the reversal potential was 3.2 ± 2 mV ($n = 10$, Fig. 1E); the second had a density and E_{rev} of -110.7 ± 10 pA/pF (Fig. 1D) and -7 ± 1 mV ($n = 12$, Fig. 1F), respectively.

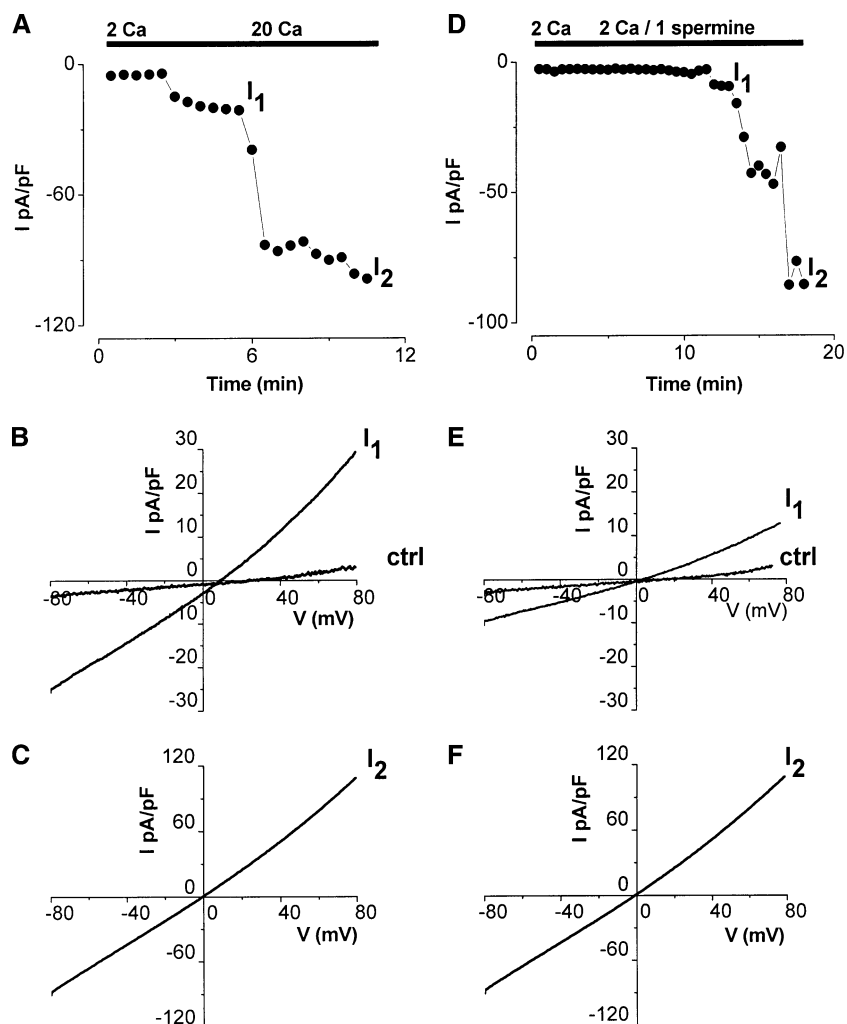


Fig. 1. CaR activation sequentially induces two cationic currents in MCF-7 cells. Time course development of $[Ca^{2+}]_o$ and spermine inward currents (measured at -80 mV) in a representative MCF-7 cell bathed in external control medium. (A) Primary current, I_1 , and secondary current, I_2 , were activated by 20 mM $[Ca^{2+}]_o$. (B) Typical current traces recorded before (Ctrl) and after (I_1) perfusion of 20 mM $[Ca^{2+}]_o$. The holding potential was -40 mV, and 250 ms voltage ramp was applied from -80 mV to $+80$ mV. (C) Typical current trace recorded during I_2 in the same experimental conditions. (D) I_1 and I_2 were activated by 1 mM spermine. (E) Typical current traces recorded before (Ctrl) and after (I_1) the extracellular perfusion of 1 mM spermine. The holding potential was -40 mV, and 250 ms voltage ramp was applied from -80 to $+80$ mV. (F) Typical current trace recorded during I_2 in 1 mM spermine.

Moreover, both 20 mM $[Ca^{2+}]_o$ and 1 mM spermine activated an outward current (Fig. 1B, C, E, F). These data show that both $[Ca^{2+}]_o$ and spermine activate CaR. This would therefore justify the interchangeable usage of the two agonists.

THE PRIMARY CURRENT MEASURED AT -80 mV IS 2-APB-SENSITIVE AND CARRIED BY Ca^{2+}

Stimulation of CaR by both $[Ca^{2+}]_o$ and spermine induced activation of PLC (Huang et al., 2002). This pathway eventually results in the activation of IP_3 store-dependent and store-independent membrane channels, both of which are thought to belong to the TRPC family (Pedersen et al., 2005; Beech, 2005).

To investigate the involvement of TRPCs in the CaR-evoked activation of the primary cationic current in MCF-7 cells, we performed a series of experiments using a number of organic and inorganic compounds, which have been shown in numerous studies to act either on endogenous cationic currents in different cell types or on the cationic currents

induced by the heterologous expression of various TRPs. The organic compounds used were 2-APB, an SOC inhibitor (Broad et al., 2001); ruthenium red (RR), a blocker of the vanilloid subfamily of TRPCs; and the most widely used of inorganic blockers, La^{3+} . Figure 2 shows that 2-APB at 50 μ M rapidly inhibited I_1 induced by both 20 mM $[Ca^{2+}]_o$ and 1 mM spermine. The average percentage blockade values of the $[Ca^{2+}]_o$ - and spermine-evoked current at -80 mV were $87.6 \pm 2\%$ ($n = 9$) and $83.6 \pm 4\%$ ($n = 9$), respectively. Moreover, I_1 was completely inhibited by 500 μ M La^{3+} ($n = 20$, data not shown), while 5 μ M RR perfusion failed to inhibit it ($n = 6$, data not shown). Furthermore, we investigated whether CaR-activated cationic channels were permeable to divalent cations, particularly Ca^{2+} . Figure 2 shows that removal of Ca^{2+} from the extracellular solution abolished the I_1 induced by both 20 mM $[Ca^{2+}]_o$ ($n = 12$, Fig. 2C) and spermine ($n = 6$, Fig. 2D), thereby suggesting that Ca^{2+} is an essential component of this current. Moreover, extracellular perfusion of Na^+ -free solution failed to reduce I_1 amplitude (data not shown, $n = 10$).

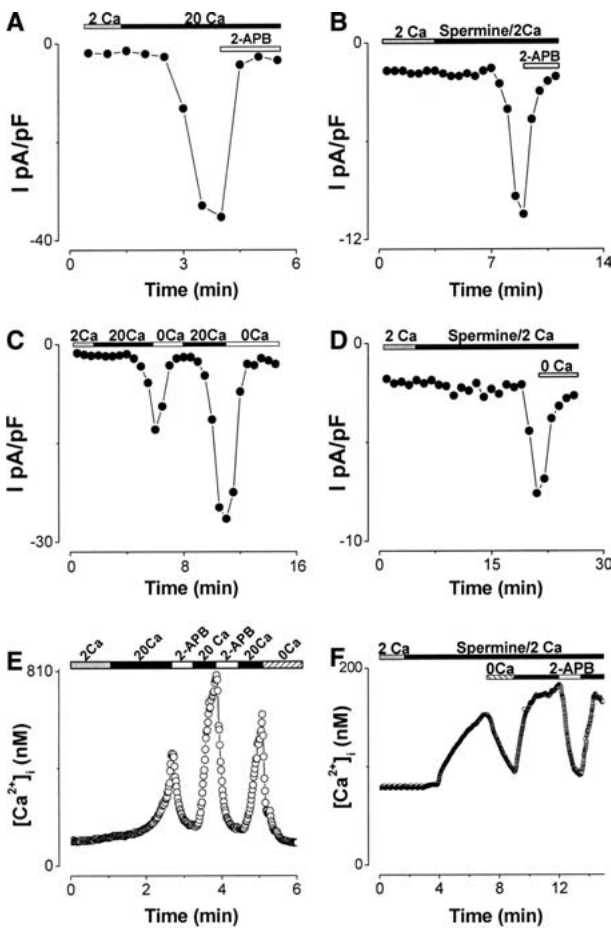


Fig. 2. 2-APB and Ca^{2+} sensitivity of $[\text{Ca}^{2+}]_o$ - and spermine-evoked primary current in MCF-7 cells. (A, B) Time courses of 20 mM $[\text{Ca}^{2+}]_o$ - and spermine-evoked inward currents (at -80 mV) in representative MCF-7 cells and responses to application of 50 μM 2-APB. (C, D) Effect of removal of extracellular Ca^{2+} on the time course of the primary inward current evoked by 20 mM $[\text{Ca}^{2+}]_o$ or 1 mM spermine. (E, F) Coapplication of cationic channel blocker 2-APB (50 μM) suppresses the 20 mM $[\text{Ca}^{2+}]_o$ - (E, $n = 41$) and 1 mM spermine- (F, $n = 54$) evoked $[\text{Ca}^{2+}]_i$ rise in MCF-7 cells. Both 20 mM $[\text{Ca}^{2+}]_o$ - and 1 mM spermine-evoked $[\text{Ca}^{2+}]_i$ increases in MCF-7 cells disappeared in nominally Ca^{2+} -free medium (0 Ca^{2+}).

To further validate the involvement of TRPCs in the CaR stimulation of MCF-7 cells, we tested the ability of 2-APB to interfere with the effect of $[\text{Ca}^{2+}]_o$ and spermine on Ca^{2+} homeostasis. An increase in $[\text{Ca}^{2+}]_o$ from 2 to 20 mM elicited an increase in $[\text{Ca}^{2+}]_i$ ($n = 41$, Fig. 2E). Perfusions of 2-APB at 50 μM reversibly blocked CaR-induced Ca^{2+} entry ($n = 41$, Fig. 2E). Moreover, removal of extracellular Ca^{2+} caused a sharp decline in $[\text{Ca}^{2+}]_i$ ($n = 41$, Fig. 2E), suggesting that virtually most of the Ca^{2+} entered the cell from the extracellular space. Perfusion of 50 μM 2-APB caused a sharp and reversible decline of the 1 mM spermine-induced $[\text{Ca}^{2+}]_i$ rise in MCF-7 cells ($n = 54$, Fig. 2F). The removal of extracellular Ca^{2+} induced a rapid decline in $[\text{Ca}^{2+}]_i$ ($n = 54$, Fig. 2F).

INVOLVEMENT OF THE PLC PATHWAY IN $[\text{Ca}^{2+}]_o$ -INDUCED INTRACELLULAR CALCIUM INCREASE

In order to prove the dependence of CaR agonist-evoked Ca^{2+} entry on the signaling cascade triggered by PLC-catalyzed phospholipid turnover, we used the PLC inhibitor U73122 and its inactive analogue U73343. Figure 3A shows that pretreatment of MCF-7 cells with 10 μM U73122 ($n = 12$) for 30 min prevented any $[\text{Ca}^{2+}]_o$ -induced $[\text{Ca}^{2+}]_i$ increase at all, whereas U73343 exerted no inhibitory effect under equivalent conditions ($n = 19$). Similar results were found in the presence of spermine (*data not shown*, $n = 6$). To further examine whether DAG-activated TRPCs make an insignificant or no contribution to the Ca^{2+} entry stimulated by CaR activation, we first treated MCF-7 cells with thapsigargin, which is known to deplete intracellular Ca^{2+} stores and thus activates SOCs, in turn promoting Ca^{2+} entry. After the thapsigargin effect, we perfused a solution containing spermine. The ability of thapsigargin to release Ca^{2+} , resulting in increased $[\text{Ca}^{2+}]_i$, is shown in Figure 3B. As store emptying induced by thapsigargin activates SOCs in the presence of 2 mM extracellular Ca^{2+} , we recorded a small Ca^{2+} entry, which is characteristic of MCF-7 cells. Spermine treatment resulted in an insignificant increase in $[\text{Ca}^{2+}]_i$. The thapsigargin effect was reported to be irreversible; thus, the SOCs remained open. In order to better visualize the Ca^{2+} entry through SOCs, we increased $[\text{Ca}^{2+}]_o$ from 2 to 20 mM and observed a large increase in $[\text{Ca}^{2+}]_i$ (Fig. 3B). Perfusion of a Ca^{2+} -free solution reduced $[\text{Ca}^{2+}]_i$ to baseline. Taken together, the PLC inhibition and thapsigargin depletion data suggest that, in contrast to SOCs, DAG-activated TRPCs make an insignificant or no contribution to the CaR response.

DOSE DEPENDENCE OF $[\text{Ca}^{2+}]_i$ AND I_1 AND I_2 CURRENT DENSITIES ON $[\text{Ca}^{2+}]_o$ -INDUCED CAR STIMULATION

The dose-response relationship for $[\text{Ca}^{2+}]_o$ -elicited increases in $[\text{Ca}^{2+}]_i$ is shown in Figure 4A. Extracellular Ca^{2+} increased $[\text{Ca}^{2+}]_i$ by $13 \pm 4\%$, $192 \pm 25\%$ and $691 \pm 60\%$ when used at 5, 10 and 20 mM, respectively. The current density of I_1 varied with the dose response of $[\text{Ca}^{2+}]_o$ (-20.5 ± 2.1 , $n = 8$, and -32.8 ± 2.6 , $n = 10$, pA/pF for 10 and 20 mM $[\text{Ca}^{2+}]_o$, respectively). The I_1 current density induced by spermine was very small (-8.7 ± 0.7 pA/pF, $n = 10$, Fig. 4B). However, the density of the second current was unvaried: -110.7 ± 10 ($n = 10$), -110.6 ± 9.4 ($n = 12$) and -118.1 ± 8.2 ($n = 13$) pA/pF for spermine, 10 mM and 20 mM $[\text{Ca}^{2+}]_o$, respectively (Fig. 4C). Taken together, these results suggest that Ca^{2+} is an essential component of the overall I_1 current, thus contributing to the fluorometrically measured $[\text{Ca}^{2+}]_o$ or spermine-induced

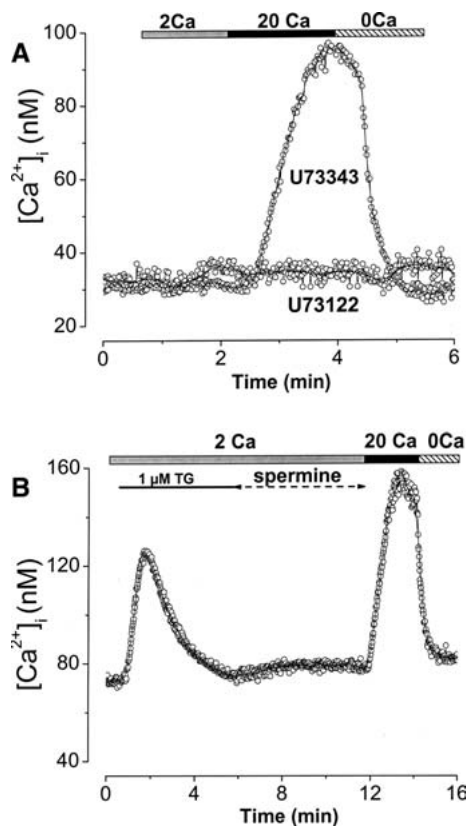


Fig. 3. Involvement of the PLC pathway in $[Ca^{2+}]_o$ -induced intracellular calcium increase. (A) Effect of extracellular Ca^{2+} is abolished in the presence of the PLC inhibitor U73122 (10 μ M, $n = 12$) and maintained in the presence of the inactive analogue U73343 (10 μ M, $n = 19$). These results are representative of the mean value. (B) The Ca^{2+} response to spermine (1 mM) is abolished when the reticulum Ca^{2+} content is previously depleted by thapsigargin (1 μ M, $n = 20$). These results are representative of the mean.

increase in $[Ca^{2+}]_i$. However, the subsequent increases in the driving force of Ca^{2+} may contribute to the I_1 amplitude. Moreover, the I_2 amplitude was unvaried in the presence of either spermine or 10 or 20 mM $[Ca^{2+}]_o$, thereby suggesting that I_2 is not affected by $[Ca^{2+}]_o$.

THE SECOND CURRENT IS Na^+ - AND Li^+ -SENSITIVE AND DEPENDENT ON THE PRIMARY ONE

As the density of the second current was so large, we suggest that this current is carried to a great extent by Na^+ ions. Replacing external Na^+ by choline reduced $77 \pm 2.7\%$ of the I_2 activated by 20 mM $[Ca^{2+}]_o$ ($n = 8$, Fig. 5A). Similar results were obtained by spermine ($n = 6$, data not shown). However, I_2 was insensitive to both 2-APB up to 75 μ M ($n = 6$, data not shown) and to 5 μ M RR ($n = 4$, data not shown). In contrast, I_2 induced by both 20 mM $[Ca^{2+}]_o$ (Fig. 5B) and spermine (Fig. 5C) was highly and reversibly inhibited by La^{3+} 500 μ M. In

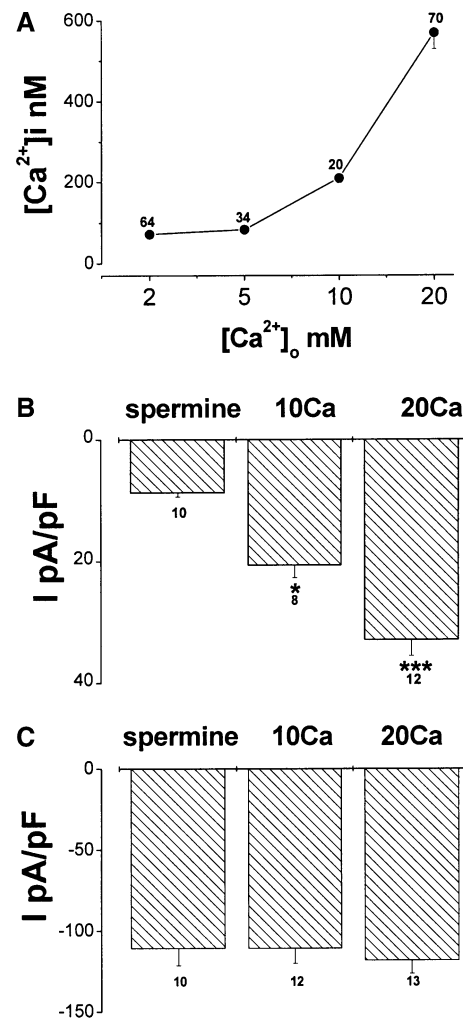


Fig. 4. Quantification of the maximal densities for $[Ca^{2+}]_o$ - and spermine-induced currents. (A) Changes in $[Ca^{2+}]_i$ upon stepwise addition of increasing $[Ca^{2+}]_o$ to MCF-7 cells. (B) Variation of I_1 amplitude according to the nature and/or concentration of the agonist used. (C) The amplitude of I_2 is stable despite the changes in the nature and/or concentrations of the agonist used. Mean \pm SE. * $P < 0.05$, *** $P < 0.001$.

order to quantify the relative permeability of Li^+ through I_2 , we replaced all Na^+ with equimolar amounts of Li^+ . Figure 5D shows representative $I-V$ coordinates derived from a ramp recording of $[Ca^{2+}]_o$ -evoked I_2 current. Li^+ is less permeable and able to carry less current than Na^+ ($n = 12$). Moreover, I_2 carried by Li^+ is completely abolished by La^{3+} 500 μ M ($n = 12$, Fig. 5D).

In order to clearly separate the two currents, we used two different protocols. Figure 6A shows the sequential time course development of 20 mM $[Ca^{2+}]_o$, which induced two inward currents at -80 mV. First, we recorded only I_1 , in Na^+ -free solution, which was completely and slowly inhibited by La^{3+} 500 μ M (Fig. 6A). The effect of La^{3+} was reversible. After the steady state of the first current was reached,

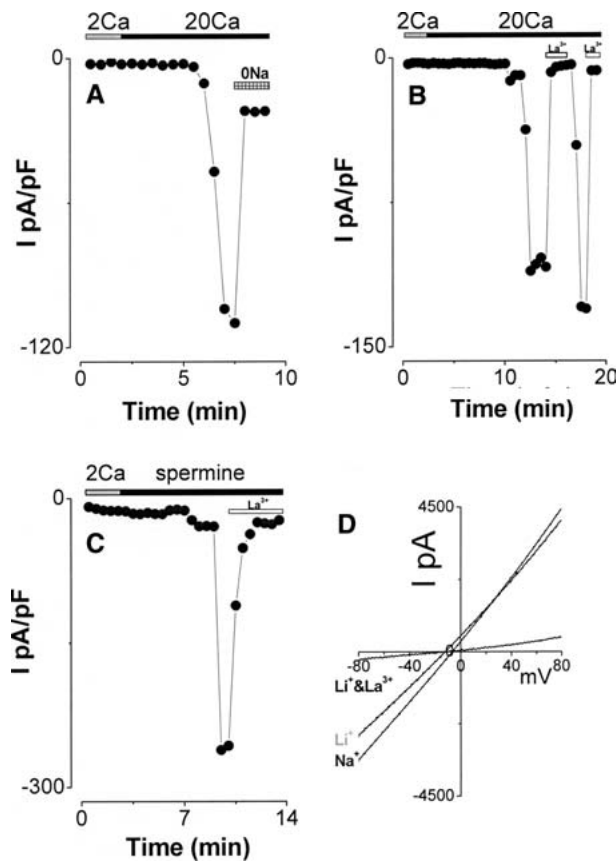


Fig. 5. Na^+ sensitivity of the inward current (I_2). (A) Removal of Na^+ dramatically reduced the 20 mM $[\text{Ca}^{2+}]_o$, which evoked the I_2 inward current. Extracellular perfusion of 500 μM La^{3+} completely inhibited I_2 induced by 20 mM $[\text{Ca}^{2+}]_o$ (B) or by 1 mM spermine (C). (D) I - V relationship of $[\text{Ca}^{2+}]_o$ -evoked I_2 in a representative cell sequentially exposed to extracellular solution containing Na^+ , Li^+ or both Li^+ and La^{3+} .

we perfused a solution containing Na^+ , which activated I_2 (Fig. 6A). The perfusion of La^{3+} induced a quick and total inhibition of I_2 (Fig. 6A). No second current was recorded in the Na^+ -free solution ($n = 40$). Second, in the control solution, both I_1 and I_2 were reversibly inhibited by 500 μM La^{3+} (Fig. 6B). Moreover, I_2 was also quickly and reversibly inhibited by a Na^+ -free medium and La^{3+} (Fig. 6B).

In all our experiments, I_2 always appeared after I_1 activation, thus suggesting a dependent relationship between these two currents. To find out if this were true, we stimulated CaR in the presence of 50 μM 2-APB. Figure 6C shows that in the presence of 2-APB no currents were activated but, as soon as we washed the 2-APB out, we induced sequential activation of I_1 followed by I_2 . Extracellular perfusion of 500 μM La^{3+} completely inhibited I_2 (Fig. 6C). These results show that I_2 is probably activated by $[\text{Ca}^{2+}]_i$. Similar results were obtained with La^{3+} (*data not shown*, $n = 10$).

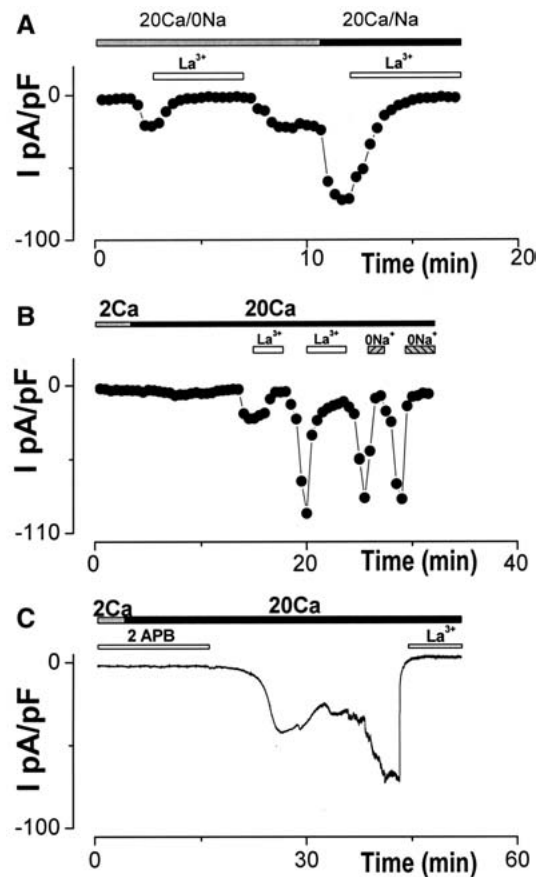


Fig. 6. Sequential activation of both currents (I_1 and I_2). (A) In the control conditions, Na^+ -free medium induced the disappearance of I_2 but not I_1 . (B) Both 500 μM La^{3+} and Na^+ -free medium inhibited I_2 current recorded at -80 mV. Moreover, I_1 current was inhibited by 500 μM La^{3+} . (C) Sequential time course development of the two 20 mM $[\text{Ca}^{2+}]_o$ -induced inward currents at -40 mV. Neither I_1 nor I_2 was activated when perfused with 2-APB (50 μM) before the activation of I_1 . However, after washout of 2-APB, we activated I_1 followed by I_2 .

PHARMACOLOGY OF I_2

As I_2 was highly permeable to Na^+ and activated after I_1 , we tested its sensitivity to flufenamic acid and Mg^{2+} , which were shown to inhibit human TRPM4, TRPM5 (Ullrich et al., 2005; Kraft & Harteneck, 2005) and transient receptor potential melastatin (TRPM) 7 (Kraft & Harteneck, 2005). Neither 100 μM internal flufenamic acid ($n = 5$, Fig. 7A) nor dialysis with high Mg^{2+} content (6 mM) ($n = 6$, Fig. 7B) inhibited I_2 . Extracellular perfusion of Na^+ -free solution or La^{3+} 500 μM inhibited this current as usual. Furthermore, internal dialysis with 100 μM spermine failed to inhibit I_2 ($n = 5$, *data not shown*).

These results demonstrate that I_2 could not be one of the TRPMs mentioned above. Moreover, as epithelial Na^+ channels are mostly expressed in epithelial-type cells, we tested the effect of amiloride.

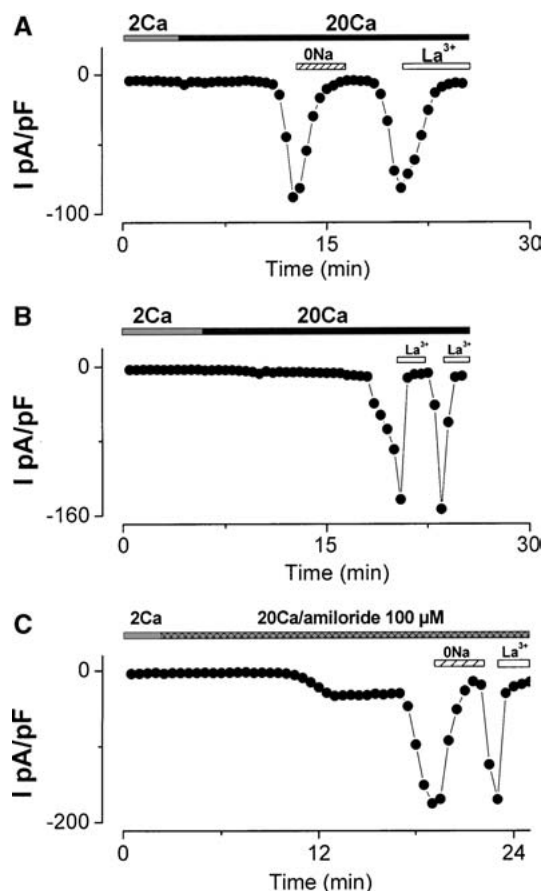


Fig. 7. Flufenamic acid, elevation of $[Mg^{2+}]_i$ and amiloride failed to inhibit the I_2 current. (A) $[Ca^{2+}]_o$ 20 mM induced I_1 and I_2 currents recorded when 100 μ M flufenamic acid was added to the intrapipette medium. Note that both 500 μ M La^{3+} and Na^+ -free solution reduced I_2 . (B) The same experiment was done in the presence of 6 mM Mg^{2+} in the patch pipette. (C) Extracellular perfusion of 100 μ M amiloride failed to inhibit I_2 . However, I_2 was sensitive to both Na^+ -free solution and 500 μ M La^{3+} .

Extracellular perfusion of amiloride 100 μ M failed to inhibit I_2 current ($n = 8$, Fig. 7C).

EXPRESSION OF PLC-COUPLED TRPCs IN MCF-7 CELLS

TRPC1-C7 are known to be involved in both the receptor-operated and store-independent Ca^{2+} entry, which is linked to the inositol phospholipid-breakdown signaling cascade (Pedersen et al., 2005). We therefore attempted to determine the potential candidates for the CaR-coupled initial current in MCF-7 cells. This was done using reverse-transcriptase (RT) PCR to analyze the expression of the specific transcripts for human isoforms of these PLC-gated TRP members in these cells. Figure 8 shows that the transcripts for the TRPC1 isoforms (Fig. 8A) and TRPC6 (Fig. 8D) were abundantly expressed in MCF-7, while TRPC3, TRPC4 and TRPC7 were undetectable (Fig. 8B, C, E). Moreover, TRPC5 was not expressed in MCF-7 cells (*data not shown*). Our

data suggest that TRPC1 and/or TRPC6 contribute to the CaR stimulation evoked by the initial current.

Discussion

CaR is expressed in the epithelial ducts of the normal human breast (VanHouten, 2005; VanHouten et al., 2004; Cheng et al., 1998). It is localized in the laterobasal membrane and interacts with ionic transporters (VanHouten, 2005). Furthermore, CaR has been characterized both in breast cancer tissue and in breast MCF-7 and MDA-MB-231 cells (Cheng et al., 1998; Sanders et al., 2000). It has also been established that CaR can regulate the production of PHTrP, which enhances MCF-7 breast cancer cell proliferation, adhesion, migration and invasion via an intracrine pathway (Rodland, 2004; Falzon & Du, 2000; Shen, Qian & Falzon, 2004). In different types of cells, including MCF-7, CaR stimulation by $[Ca^{2+}]_o$ or spermine elicits an increase in $[Ca^{2+}]_i$ (Nemeth & Scarpa, 1987; Parkash et al., 2004). Furthermore, CaR stimulation is accompanied by PLC stimulation and IP_3 production (Brown et al., 1987; Brown & MacLeod, 2001; Huang et al., 2002; Jiang et al., 2002). In this study, we present, for the first time, evidence of the role of CaR in Ca^{2+} signaling in MCF-7 cells. Furthermore, we show that the CaR-stimulated Ca^{2+} transmembrane influx was followed by an Na^+ one and that activation of these currents may involve a store-dependent and/or independent mechanism.

Our results support a role of CaR in MCF-7 cells, an estrogen-positive human breast cancer cell line, in sensing and responding to change in $[Ca^{2+}]_o$ (Figs. 2 and 3). A nonoscillatory response was observed in MCF-7 cells instead of the $[Ca^{2+}]_i$ oscillations that were observed in HEK293 cells expressing CaR (Jiang et al., 2002). Moreover, our results are similar to those reported in MCF-7 by Parkash et al. (2004), who found a median effective concentration (EC_{50}) of about 21 mM.

It has been reported that CaR activation by neomycin, spermine or elevated $[Ca^{2+}]_o$ induces activation of nonselective cationic channels (Ye et al., 1996a, 1997; Chattopadhyay et al., 2000). More recently, Fatherazi et al. (2004) reported that in gingival cells CaR activation by 10 mM $[Ca^{2+}]_o$ induced activation of two cationic currents (at -80 mV). Both currents are supported by Ca^{2+} influx. The present whole-cell patch-clamp results show that CaR activation sequentially induced two cationic currents, the first being highly Ca^{2+} -sensitive followed by a second Na^+ one. Our first current closely resembles the second current reported by Fatherazi et al. (2004). However, no Na^+ current was recorded by Fatherazi et al. (2004). Our second current seems to be dependent on $[Ca^{2+}]_i$ since it was always activated after the

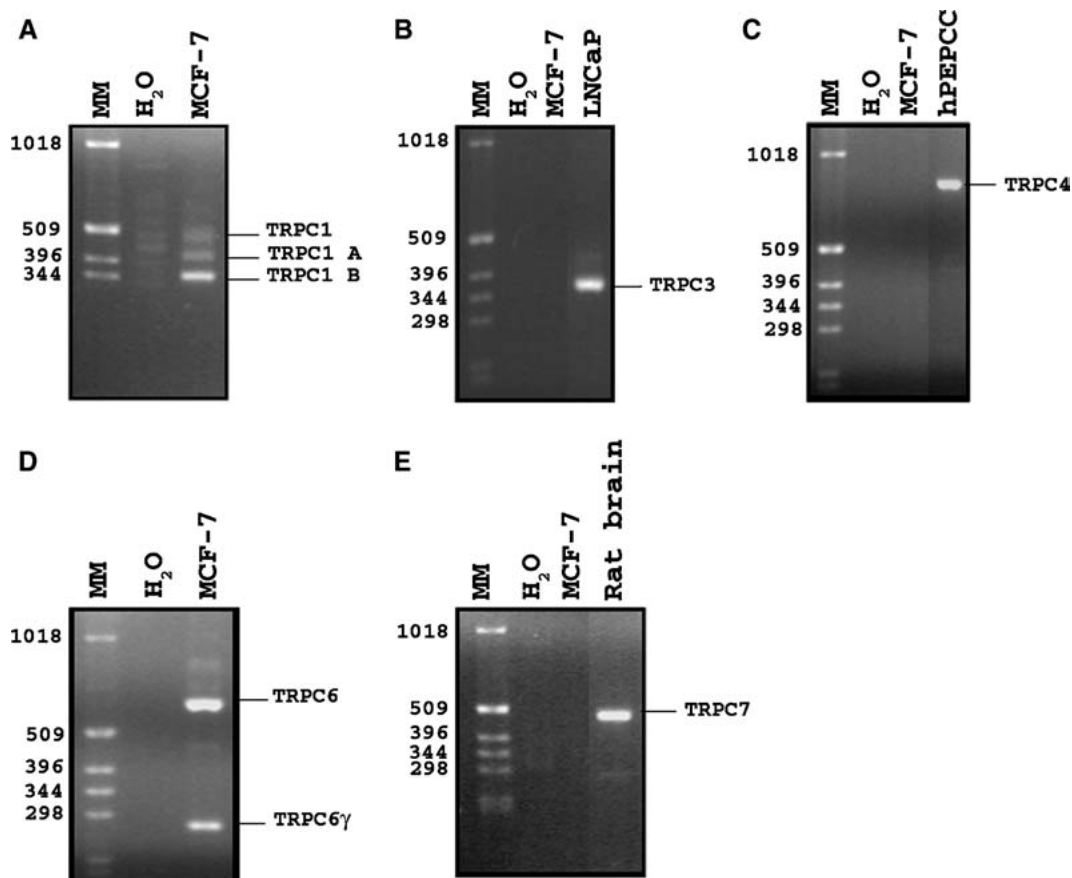


Fig. 8. Expression of CaR coupled to members of the TRPC family in MCF-7 cells. RT-PCR analysis of the expression of human TRPC1 (A), TRPC3 (B), TRPC4 (C), TRPC6 (D) and TRPC7 (E) transcripts in MCF-7 cells. Expression products were obtained using the primers described in the text. Human prostate cancer epithelial cell line LNCaP, human primary epithelial prostate cancer cell line hPEPCC, and rat brain cells were used as positive controls for the detection of TRPC3, TRPC4 and TRPC7, respectively. H₂O, negative controls; MM, molecular weight marker.

I_1 current. This channel is nonselective since it conducts Li^+ , Na^+ and Cs^+ . It was inhibited by neither high Mg^{2+} , flufenamic acid nor spermine dialysis, thus suggesting that the channel is not a member of the reported TRPM 4, 5, 7 family. However, we do not exclude the involvement of other TRPM-like channels yet to be identified. Moreover, I_2 was insensitive to amiloride (100 μM), excluding the involvement of Na^+ -epithelial channels. The increase in $[\text{Ca}^{2+}]_i$ may also activate an $\text{Na}^+/\text{Ca}^{2+}$ exchanger, thereby inducing Na^+ entry. However, the large amplitude of the second current excludes this hypothesis.

Our study provides direct evidence that CaR is functionally coupled to transmembrane Ca^{2+} entry via the PLC-catalyzed inositol phospholipid-breakdown signaling pathway, presumably through activation of channels of the TRP family. IP_3 and DAG are two factors which are probably involved in Ca^{2+} entry in response to CaR stimulation by agonists. The first is related to the IP_3 -evoked depletion of intracellular Ca^{2+} stores and the subsequent activation of plasmalemmal SOCs, also thought to belong

to the TRPC family (Pedersen et al., 2005; Parekh & Putney, 2005). The second, however, is related to direct DAG-mediated activation of other TRP members (Pedersen et al., 2005).

Our results show that MCF-7 cells pretreated with U73122 (a specific inhibitor of PLC) abolished the $[\text{Ca}^{2+}]_o$ -stimulated $[\text{Ca}^{2+}]_i$ increase, indicating that both store-dependent and independent TRPs are involved in the CaR response. Moreover, RT-PCR analysis showed the presence of the specific mRNA for only TRPC1 and TRPC6. The details of the molecular nature of the primary Ca^{2+} -sensitive channel remain to be explored. However, a number of observations argue that the underlying cationic channels are closely related to SOCs. (1) 2-APB at low concentrations is capable of blocking nearly 100% of CaR-induced I_1 and $[\text{Ca}^{2+}]_i$; (2) the CaR-induced I_1 current is insensitive to RR, a potent inhibitor of such members of the transient receptor potential vanilloid (TRPV) family; and (3) spermine had no effect after treatment with thapsigargin, suggesting that there was no involvement of a TRP family member activated by DAG. Moreover, a

correlation with the permeation and pharmacological profiles of the first cationic current, I_1 , in MCF-7 cells with those described for TRPC6 shows a number of notable differences: (1) I_1 was highly permeable to Ca^{2+} , in contrast to TRPC6 which is permeable to Ca^{2+} and Na^+ ; (2) the increase in $[\text{Ca}^{2+}]_o$ increased I_1 amplitude, while it reduced TRPC6 activity; and (3) dialysis with 100 μM flufenamic acid, a TRPC6 activator, was without effect on I_1 . Taken together, these findings suggest that the CaR-activated cationic channels in MCF-7 cells are probably heterotetramultimers that necessarily include both TRPC6 and TRPC1 together with some other TRP members, which confer the property of SOC gating and, in combination, determine the resultant permeation and pharmacological characteristics of the whole channel.

Changes in $[\text{Ca}^{2+}]_i$ are known to play an important role in the regulation of PTHrP secretion by MCF-7 cells (Brown et al., 1993). The MCF-7 cell line expresses functional PTH/PTHrP receptors, and PTHrP affects its growth in an autocrine/paracrine manner (Liapis et al., 1993). In this way, the CaR-induced TRP activation (store-dependent and/or independent) permits Ca^{2+} influx and an increase in $[\text{Ca}^{2+}]_i$. Moreover, the Na^+ entry by a nonselective cation channel, which could be a member of the TRPM family, may induce an inverse function of the $\text{Na}^+/\text{Ca}^{2+}$ exchanger, thereby causing an additional Ca^{2+} entry, which allows a sustained increase in $[\text{Ca}^{2+}]_i$ and the secretion of PTHrP and/or changes in gene expression, such as estrogen receptor downregulation in MCF-7 cells (Journe et al., 2004).

In conclusion, our findings provide new information about nonselective cationic channels supporting CaR-activated Ca^{2+} influx pathways in MCF-7 cells. These findings therefore contribute to the understanding of the functional significance of the presence of CaR in breast cancer cells.

We thank Jean François Lefebvre and Philippe Delcourt for their excellent technical assistance. This work was supported by the Ministère de l'Éducation Nationale, the Ligue Nationale Contre le Cancer, the Association pour la Recherche Contre le Cancer and the Region Picardie, France and by grants from Morocco.

References

- Beech, D.J 2005. TRPC1: Store-operated channel and more. *Pfluegers Arch.* **451**:53–60
- Boring, C.C., Squire, T.S., Tong, T., Montgomery, S 1994. Cancer statistics. *CA Cancer J. Clin.* **44**:7–26
- Broad, L.M., Braun, F.J., Lievreumont, J.P., Bird, G.S., Kurosaki, T., Putney, J.W., Jr 2001. Role of the phospholipase C-inositol 1,4,5-trisphosphate pathway in calcium release-activated calcium current and capacitative calcium entry. *J. Biol. Chem.* **276**:15945–15952
- Brown, E.M., Enyedi, P., LeBoff, M., Rotberg, J., Preston, J., Chen, C 1987. High extracellular Ca^{2+} and Mg^{2+} stimulate accumulation of inositol phosphates in bovine parathyroid cells. *FEBS Lett.* **218**:113–138
- Brown, E.M., Gamba, G., Ricciardi, D., Lombardi, M., Butters, R., Kifor, O., Sun, A., Hediger, M.A., Lytton, J., Hebert, S.C 1993. Cloning and characterization of an extracellular Ca^{2+} -sensing receptor from bovine parathyroid. *Nature* **366**:575–580
- Brown, E.M., MacLeod, R.J 2001. Extracellular calcium sensing and extracellular calcium signalling. *Physiol. Rev.* **81**:239–297
- Buchs, N., Manen, D., Bonjour, J.P., Rizzoli, R 2000. Calcium stimulates parathyroid hormone-related protein production in Leydig tumor cells through a putative cation-sensing mechanism. *Eur. J. Endocrinol.* **142**:500–505
- Chattopadhyay, N., Evliyaoglu, C., Heese, O., Carroll, R., Sanders, J., Black, P., Brown, E.M 2000. Regulation of secretion of PTHrP by Ca^{2+} -sensing receptor in human astrocytes, astrocytomas, and meningiomas. *Am. J. Physiol.* **279**:C691–C699
- Cheng, I., Klingensmith, M.E., Chattopadhyay, N., Kifor, O., Butters, R.R., Soybel, D.I., Brown, E.M 1998. Identification and localization of the extracellular calcium-sensing receptor in human breast. *J. Clin. Endocrinol. Metab.* **83**:703–707
- Falzon, M., Du, P 2000. Enhanced growth of MCF-7 breast cancer cells overexpressing parathyroid hormone-related peptide. *Endocrinology* **141**:1882–1892
- Fatherazi, S., Belton, C.M., Cai, S., Zarif, S., Goodwin, P.C., Lamont, R.J., Izutsu, K.T 2004. Calcium receptor message, expression and function decrease in differentiating keratinocytes. *Pfluegers Arch.* **448**:93–104
- Guisse, T.A., Yin, T.A., Taylor, S.D., Kumagai, Y., Dallas, M., Boyce, B.F., Yoneda, T., Mundy, G.R 1996. Evidence for a causal role of parathyroid hormone-related protein in the pathogenesis of human breast cancer-mediated osteolysis. *J. Clin. Invest.* **98**:1544–1549
- Huang, C., Handlogten, M.E., Miller, R.T 2002. Parallel activation of phosphatidylinositol 4-kinase and phospholipase C by the extracellular calcium-sensing receptor. *J. Biol. Chem.* **277**:20293–20300
- Jiang, Y.F., Zhang, Z., Kifor, O., Lane, C.R., Suinn, S.J., Bai, M 2002. Protein kinase C (PKC) phosphorylation of the Ca^{2+} -sensing receptor (CaR) modulates functional interaction of G proteins with the CaR cytoplasmic tail. *J. Biol. Chem.* **277**:50543–50549
- Journe, F., Dumon, J.C., Kheddoumi, N., Fox, J., Laios, I., Leclercq, G., Body, J.J 2004. Extracellular calcium downregulates estrogen receptor alpha and increases its transcriptional activity through calcium-sensing receptor in breast cancer cells. *Bone* **35**:479–488
- Kraft, R., Harteneck, C 2005. The mammalian melastatin-related transient receptor potential cation channels: An overview. *Pfluegers Arch.* **451**:204–211
- Li, S., Huang, S., Peng, S.B 2005. Overexpression of G protein-coupled receptors in cancer cells: Involvement in tumor progression. *Int. J. Oncol.* **27**:1329–1338
- Liapis, H., Crouch, E.C., Grosso, L.E., Kitazawa, S., Wick, M.R 1993. Expression of parathyroidlike protein in normal, proliferative, and neoplastic human breast tissues. *Am. J. Pathol.* **174**:1169–1178
- Mundy, G.R 1997. Mechanisms of bone metastasis. *Cancer* **80**:1546–1556
- Nemeth, E.F., Scarpa, A 1987. Rapid mobilization of cellular Ca^{2+} in bovine parathyroid cells evoked by extracellular divalent cations. Evidence for a cell surface calcium receptor. *J. Biol. Chem.* **262**:5188–5196
- Ouadid-Ahidouch, H., Roudbaraki, M., Delcourt, P., Ahidouch, A., Joury, N., Prevarskaya, N 2004. Functional and molecular identification of intermediate-conductance Ca^{2+} -activated K^+ channels in breast cancer cells: Association with cell cycle progression. *Am. J. Physiol.* **287**:C125–C134

- Parekh, A.B., Putney, J.W., Jr 2005. Store-operated calcium channels. *Physiol. Rev.* **85**:757–810
- Parkash, J., Chaudhry, M.A., Rhoten, W.B 2004. Calbindin-D28k and calcium sensing receptor cooperate in MCF-7 human breast cancer cells. *Int. J. Oncol.* **24**:1111–1119
- Pedersen, S.F., Owsianik, G., Nilius, B 2005. TRP channels: An overview. *Cell Calcium* **38**:233–252
- Rodland, K.D 2004. The role of the calcium-sensing receptor in cancer. *Cell Calcium* **35**:291–295
- Sanders, J.L., Chattopadhyay, N., Kifor, O., Yamaguchi, T., Butter, R.R., Brown, E.M 2000. Extracellular calcium-sensing receptor expression and its potential role in regulating parathyroid hormone-related peptide secretion in human breast cancer cell lines. *Endocrinology* **141**:4357–4364
- Sanders, J.L., Chattopadhyay, N., Kifor, O., Yamaguchi, T., Butter, R.R., Brown, E.M 2001. Ca²⁺-sensing receptor expression and PTHrP secretion in PC-3 human prostate cancer cells. *Am. J. Physiol.* **281**:E1267–E1274
- Shen, X., Qian, L., Falzon, M 2004. PTH-related protein enhances MCF-7 breast cancer cell adhesion, migration, and invasion via an intracrine pathway. *Exp. Cell. Res.* **294**:420–433
- Silver, I.A., Murrills, R.J., Etherington, D.J 1988. Microelectrode studies on the acid microenvironment beneath adherent macrophages and osteoclast. *Exp. Cell. Res.* **175**:266–276
- Ullrich, N.D., Voets, T., Prenen, J., Vennekens, R., Talavera, K., Droogmans, G., Nilius, B 2005. Comparison of functional properties of the Ca²⁺-activated cation channels TRPM4 and TRPM5 from mice. *Cell Calcium* **37**:267–278
- VanHouten, J.N 2005. Calcium sensing by the mammary gland. *Neoplasia* **10**:129–139
- VanHouten, J.N., Danna, P., McGeoch, G., Brown, E.M., Krapcho, K., Neville, M., Wysolmerski, J.J 2004. The calcium-sensing receptor regulates mammary gland parathyroid hormone-related protein production and calcium transport. *J. Clin. Invest.* **113**:598–608
- Yamaguchi, T., Ye, C., Chattopadhyay, N., Sanders, J.L., Vassilev, P.M., Brown, E.M 2000. Enhanced expression of extracellular calcium sensing receptor in monocyte-differentiated versus undifferentiated HL-60 cells: Potential role in regulation of a nonselective cation channel. *Calcif. Tissue Int.* **66**:375–382
- Ye, C.P., Kanazirska, M., Quinn, S., Brown, E.M., Vassilev, P.M 1996a. Modulation by polycationic Ca²⁺-sensing receptor agonists of nonselective cation channels in rat hippocampal neurons. *Biochem. Biophys. Res. Commun.* **224**:271–280
- Ye, C.P., Rogers, K., Bai, M., Quinn, S., Seidman, C.E., Seidman, J.G., Brown, E.M., Vassilev, P.M 1996b. Agonists of the Ca²⁺-sensing receptor (CaR) activate nonselective cation channels in HEK293 cells stably transfected with the human CaR. *Biochem. Biophys. Res. Commun.* **226**:272–279
- Ye, C.P., Ho-Pao, C.L., Kanazirska, M., Quinn, S., Rogers, K., Seidman, C.E., Seidman, J.G., Brown, E.M., Vassilev, P.M 1997. Amyloid-beta proteins activate Ca²⁺-permeable channels through calcium-sensing receptors. *J. Neurosci. Res.* **47**:547–554
- Zitt, C., Halaszovich, C.R., Luckhoff, A 2002. The TRP family of cation channels: Probing and advancing the concepts on receptor-activated calcium entry. *Prog. Neurobiol.* **66**:243–264